J. Fluid Mech. (1967), *vol.* 30, *part* 3, *pp.* 449–464
Printed in Great Britain

Laminar and transitional flow of drilling muds and various suspensions in circular tubes

By BERNARD LE FUR
Laboratoire d'Aérothermique du C.N.R.S., Meudon, France
AND MADELEINE MARTIN
Institut Français du Pétrole, Rueil-Malmaison, France

(Received 28 November 1966 and in revised form 10 May 1967)

Most suspensions exhibit a rheological behaviour which cannot be represented by either Bingham's or Ostwald–De Waele's law. In studying such cases a very simple expression with only three parameters may be used. Starting with an intermediate law of this sort, this paper gives velocity profiles and head losses in laminar flow, which have been computed and plotted on diagrams in non-dimensional co-ordinates.

It has been found that transition flow rates in circular tubes for data taken from the literature and from experiments conducted on drilling muds at the Institut Français du Pétrole, are efficiently predicted by an empirical criterion (Ryan & Johnson 1959) which establishes a relation between a generalized Reynolds number and a generalized Hedström number.

1. Rheological relationships

Engineers interested in problems relating to the flow of muds in circular or annular conduits during the process of drilling, usually simplify the rheological behaviour of the medium by assuming the validity of Bingham's law or that of Ostwald and De Waele (see, for instance, Melrose & Lilienthal 1951). On closer examination, it appears that neither law is capable of fully describing the behaviour of drilling muds or other suspensions such as cement slurries, greases, etc. Figures 1 and 2 show clearly that the experimental curve for a typical drilling mud does not conform either to Bingham's law (straight line in the diagram of figure 1), or to Ostwald–De Waele's law (straight line in the diagram of figure 2). Various constitutive equations have been proposed to represent such fluids (Casson 1959; Sisko 1958; Powell & Eyring 1944; Herschel & Bulkley 1926; Briant 1956, etc.). All except Casson introduce three parameters for the sake of better data representation.

With the aid of the formulas given by Krieger & Maron (1954), it is possible to obtain a rheological relationship between the shear stress τ and the shear rate $\dot{\gamma}$ from the torques measured at various speeds using coaxial-cylinder viscometers. We have found that the rheological law introduced by Briant (1956),

$$\tau = \tau(\dot{\gamma}) = \mu_\infty \dot{\gamma}(1 + \tau_\infty/m\mu_\infty\dot{\gamma})^m, \tag{1}$$

satisfactorily represents experimental data in the investigated range, where m is a non-dimensional parameter, τ_∞ has the dimensions of shear stress and μ_∞ the dimensions of viscosity.

Equation (1) can be put in a non-dimensional form by introducing a reduced shear rate

$$\dot{\gamma}^* = m\mu_\infty\dot{\gamma}/\tau_\infty, \tag{2}$$

and a reduced shear stress

$$\tau^* = m\tau/\tau_\infty; \tag{3}$$

this gives

$$\tau^* = \dot{\gamma}^{*1-m}(1+\dot{\gamma}^*)^m. \tag{4}$$

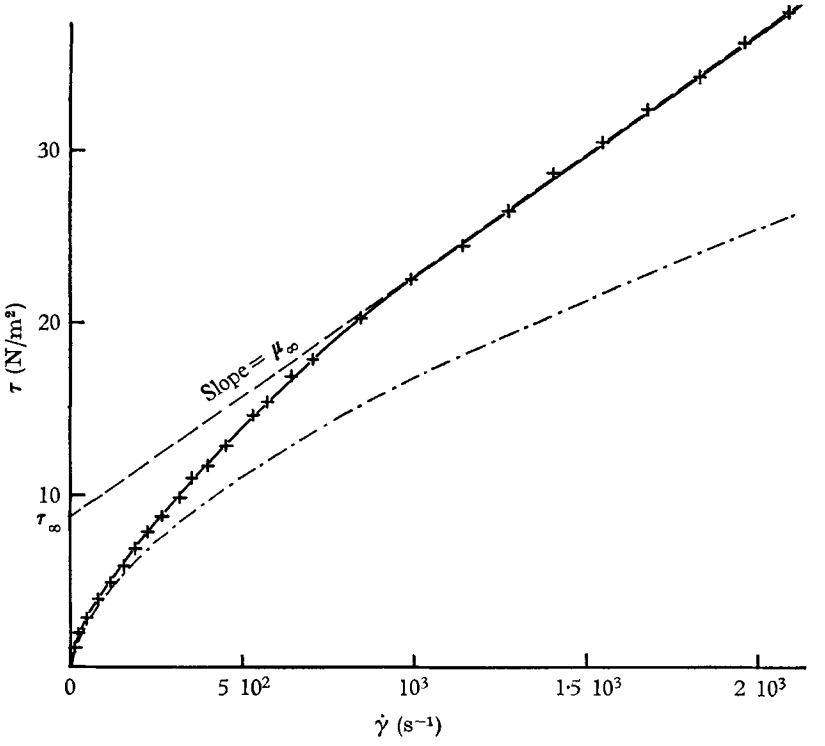

FIGURE 1. Diagram for a drilling mud with rheological parameters: $m = 0{\cdot}4$, $\tau_\infty = 8{\cdot}8$ N/m², $\mu_\infty = 0{\cdot}014$ Pl. ———, experimental curve; — — —, Bingham fluid having same asymptotic behaviour as $\dot{\gamma} \to \infty$; — · — · —, Ostwald–De Waele fluid having same behaviour as $\dot{\gamma} \to 0$.

This relation is shown diagrammatically in figure 3 as a family of curves for $\log\tau^*$ vs. $\log\dot{\gamma}^*$. This diagram allows us to determine the values of m, τ_∞ and μ_∞ from experimental results obtained in coaxial-cylinder viscometers. This is done by plotting the experimental points on transparent paper in the form of a logarithmic diagram, using the same scale as in figure 3. The transparent diagram is then placed on top of figure 3 and moved until the points lie on one of the curves or on an interpolated curve between two curves of figure 3. This is shown in figure 2, from which can be determined the value a of the shearing stress corresponding to $\tau^* = 1$ and the value b of the shear rate corresponding to $\dot{\gamma}^* = 1$. It is seen that

$$\tau_\infty = ma, \quad \mu_\infty = a/b. \tag{5}$$

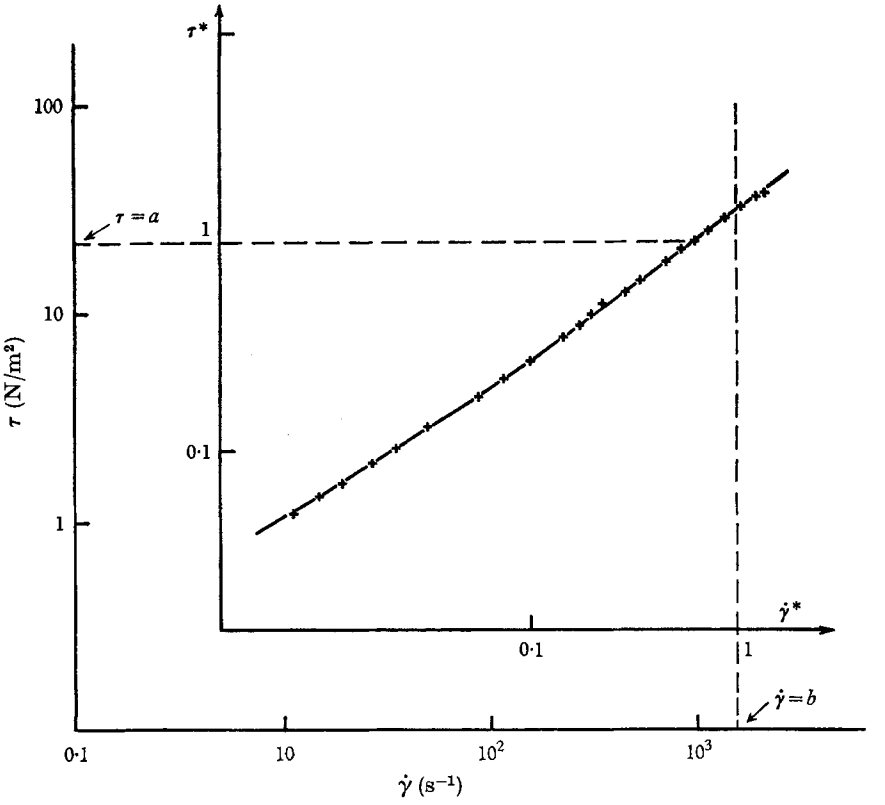

FIGURE 2. Log τ, log $\dot{\gamma}$ diagram for the same drilling mud as in figure 1 showing determination of its rheological parameters using figure 3.

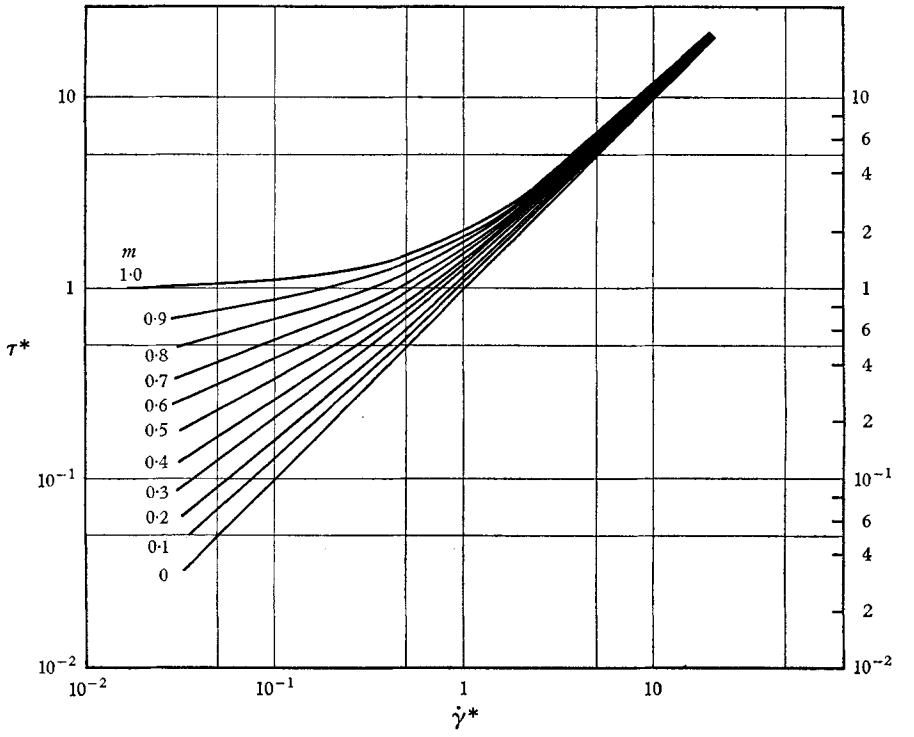

FIGURE 3. Calculated (log τ^*, log $\dot{\gamma}^*$) diagram for different values of m.

A further example is given in figure 4, for drilling mud. The values of the rheological parameters are (using M.K.S. units)

$$m = 0{\cdot}8, \quad \tau_\infty = 3{\cdot}32\,\mathrm{N/m^2} \quad \text{and} \quad \mu_\infty = 0{\cdot}0078\,\mathrm{Pl}.$$

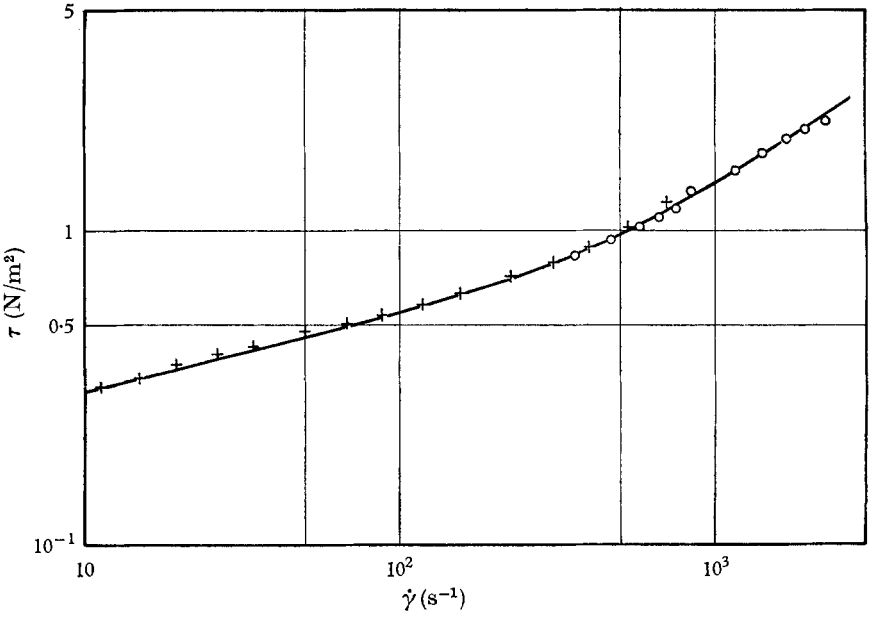

FIGURE 4. Characteristic curve for a drilling mud: $m = 0{\cdot}8$, $\tau_\infty = 3{\cdot}32$ N/m², $\mu_\infty = 0{\cdot}0078$ Pl. +, From coaxial viscometer with a gap of 0·0119 cm; ○, from coaxial viscometer with a gap of 0·0130 cm.

2. Laminar flow in a circular conduit

Because very low torques cannot be accurately measured on viscometers, we have used (1), not only as an interpolation but also as an extrapolation formula for the lower values of shear stresses, in order to calculate velocity profiles and head losses in laminar flow in a circular conduit. As low values of shear stress are found only in the near-axis region, the guessing of shear rates has a non-negligible influence on the form of velocity profiles and hence on the flow rate, the pressure gradient being given. The validity of the extrapolation will be examined *a posteriori* by comparing the calculated head losses with the experimental results.

By applying the momentum theorem, it is possible to show that the tangential stress in a fluid flowing through a circular pipe of radius R is given by

$$\tau(r) = r\tau_R/R, \tag{6}$$

where τ_R stands for $\tau(R)$, and r is the local radial co-ordinate.

If we assume the velocity $u(R)$ at the wall of the tube to be zero, the fluid velocity is given by

$$u(r) = \int_r^R \dot{\gamma}\,dr = \frac{R}{\tau_R}\int_{\tau(r)}^{\tau(R)} \dot{\gamma}\,d\tau. \tag{7}$$

Using the reduced variables (2) and (3), we obtain

$$u(r) = \frac{R\tau_\infty}{m\mu_\infty \tau_R^*} \int_{\tau^*}^{\tau_R^*} \dot{\gamma}^* d\tau^*, \tag{8}$$

and, on integration by parts,

$$u(r) = \frac{R\tau_\infty}{m\mu_\infty \tau_R^*} \left[|\tau^*\dot{\gamma}^*|_{\dot{\gamma}^*}^{\dot{\gamma}_R^*} - \int_{\dot{\gamma}^*}^{\dot{\gamma}_R^*} \tau^* d\dot{\gamma}^* \right], \tag{9}$$

where $$\dot{\gamma}_R^* \equiv \dot{\gamma}^*(R).$$

Using (4), the integral $$\int_{\dot{\gamma}^*}^{\dot{\gamma}_R^*} \tau^* d\dot{\gamma}^*$$

can be put in the form

$$\int_{\dot{\gamma}^*}^{\dot{\gamma}_R^*} \dot{\gamma}^{*1-m}(1+\dot{\gamma}^*)^m d\dot{\gamma}^* = \int_0^{\dot{\gamma}_R^*} \sigma^{1-m}(1+\sigma)^m d\sigma - \int_0^{\dot{\gamma}^*} \sigma^{1-m}(1+\sigma)^m d\sigma. \tag{10}$$

In these integrals, we put

$$\sigma = \frac{av}{1+a(1-v)}. \tag{11}$$

Then $$\int_0^a \sigma^{1-m}(1-\sigma)^m d\sigma = \left(\frac{a}{a+1}\right)^{2-m} \int_0^1 v^{1-m}\left(1-\frac{va}{1+a}\right)^{-3} dv$$

$$= \frac{1}{2-m}\left(\frac{a}{a+1}\right)^{2-m} {}_2F_1\left(3, 2-m; 3-m; \frac{a}{1+a}\right),$$

where ${}_2F_1$ is the hypergeometric function defined by the series

$${}_2F_1(\alpha, \beta; \gamma; x) = \frac{\Gamma(\gamma)}{\Gamma(\alpha)\Gamma(\beta)} \sum_{n=0}^{\infty} \frac{\Gamma(\alpha+n)\Gamma(\beta+n)}{\Gamma(\gamma+n)} \frac{x^n}{n!}. \tag{12}$$

This series converges for $|x| < 1$ and the function can also be expressed in the form of the definite integral

$${}_2F_1(\alpha, \beta; \gamma; x) = \frac{\Gamma(\gamma)}{\Gamma(\beta)\,\Gamma(\gamma-\beta)} \int_0^1 v^{\beta-1}(1-v)^{\gamma-\beta-1}(1-vx)^{-\alpha} dv, \tag{13}$$

if $$\mathrm{Re}(\beta) > 0 \quad \text{and} \quad \mathrm{Re}(\gamma-\beta) > 0.$$

Finally, the velocity is given in the following parametric form:

$$\left.\begin{aligned} u &= (R\tau_\infty/m\mu_\infty)\,\dot{\gamma}_R^{*m-1}(1+\dot{\gamma}_R^*)^{-m}[P(\dot{\gamma}_R^*) - P(\dot{\gamma}^*)], \\ r &= R\left(\frac{\dot{\gamma}^*}{\dot{\gamma}_R^*}\right)^{1-m}\left(\frac{1+\dot{\gamma}^*}{1+\dot{\gamma}_R^*}\right)^m, \end{aligned}\right\} \tag{14}$$

with $\dot{\gamma}^*$ denoting the parameter. Here, the function P is defined as

$$P(\dot{\gamma}^*) \equiv \dot{\gamma}^{*2-m}(1+\dot{\gamma}^*)^m - \frac{1}{2-m}\left(\frac{\dot{\gamma}^*}{1+\dot{\gamma}^*}\right)^{2-m} {}_2F_1(3, 2-m; 3-m; \dot{\gamma}^*/(1+\dot{\gamma}^*)). \tag{15}$$

Head losses per unit length

Head losses per unit length are given by

$$\Delta\hat{p}/L = 2\tau_R/R \tag{16}$$

where L is the length of the pipe and the driving pressure is

$$\hat{p} = p + \rho g z,$$

z being a vertical co-ordinate, g gravity and ρ the fluid density. The friction factor, f, is, by definition,

$$f = \frac{4R}{\rho\bar{u}^2}\frac{\Delta\hat{p}}{L} = \frac{8\tau_R}{\rho\bar{u}^2}, \tag{17}$$

where $\bar{u}$ is the mean velocity defined by

$$\bar{u} = \frac{2}{R^2}\int_0^R ru\,dr. \tag{18}$$

Using dimensional analysis, it is possible to show that the friction factor is a function of two non-dimensional numbers when the fluid is non-Newtonian in the sense of equation (1).

We introduce here a generalized Reynolds number

$$Re = \rho\bar{u}D/\mu_\infty, \tag{19}$$

and a generalized Hedström number

$$He = D^2\rho\tau_\infty/m\mu_\infty^2, \tag{20}$$

where $D = 2R$ is the tube diameter.

In *laminar flow*, Martin & Le Fur (1963) have shown that the friction factor takes a special form:

$$f(Re, He) = (8He/Re^2)\,\Phi(Re/He), \tag{21}$$

where the function Φ is related to the expression for τ^* as a function of $\dot{\gamma}^*$. If we plot the reduced pressure gradient in terms of

$$\tilde{f} = f\frac{Re^2}{He} = \frac{2mD}{\tau_\infty}\frac{\Delta\hat{p}}{L} = \frac{8m\tau_R}{\tau_\infty} \tag{22}$$

as a function of a new non-dimensional number

$$N = \frac{Re}{He} = \frac{m(\bar{u}/D)}{\tau_\infty}\mu_\infty = \frac{4m\mu_\infty q}{\pi D^3\tau_\infty}, \tag{23}$$

q being the flow rate, we obtain a single curve for all tube diameters. The coefficient $\tilde{f}$ may be interpreted as being proportional to the ratio between the wall shear stress and the characteristic shear stress of the liquid. The number N is the reduced volume flow rate. For Bingham bodies, it would be inversely proportional to the number introduced by Prager (1961).

By calculating the mean velocity $\bar{u}$ from equations (14), the following parametric relation between N and $\tilde{f}$ is obtained:

$$\left.\begin{aligned} \tilde{f} &= 8\dot{\gamma}_R^{*1-m}(1+\dot{\gamma}_R^*)^m, \\ N &= \frac{\dot{\gamma}_R^*}{6} - \frac{\dot{\gamma}_R^*}{6(4-3m)\,(1+\dot{\gamma}_R^*)^4}\,{}_2F_1\left(5, 4-3m; 5-3m; \frac{\dot{\gamma}_R^*}{1+\dot{\gamma}_R^*}\right). \end{aligned}\right\} \tag{24}$$

Log $\tilde{f}$ is shown, for different values of the parameter m, as a function of log N in figure 5. If we now introduce the reduced radius

$$r^* = \tfrac{1}{8}\tilde{f}r/R,$$

and the reduced velocity $$u^* = \tfrac{1}{4}\tilde{f}Nu/\bar{u},$$

we can obtain a diagram from which it is easy to deduce the velocity profiles.

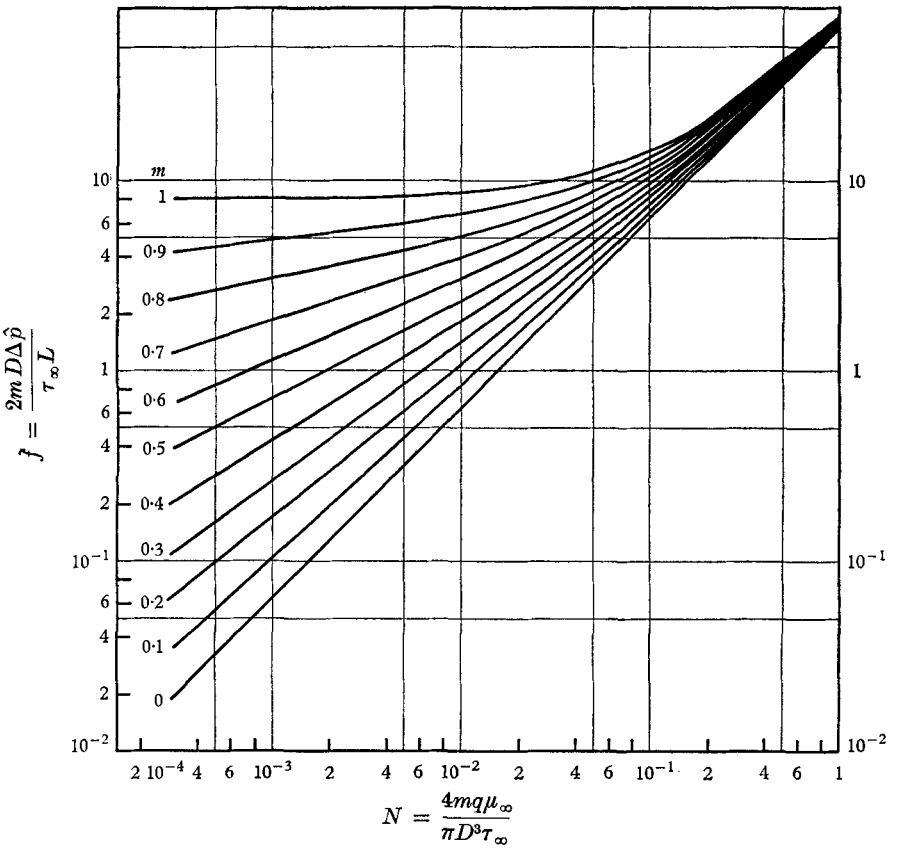

FIGURE 5. (log $\tilde{f}$, log N) calculated for different values of m.

The reduced velocity defect Δu^* is a parametric function of the reduced radius

$$\Delta u^* = u_M^* - u^* = P(\dot{\gamma}^*)$$
$$= \dot{\gamma}^{*2-m}(1+\dot{\gamma}^*)^m - \frac{1}{2-m}\left(\frac{\dot{\gamma}^*}{1+\dot{\gamma}^*}\right)^{2-m} {}_2F_1\left(3, 2-m; 3-m; \frac{\dot{\gamma}^*}{1+\dot{\gamma}^*}\right),$$
$$r^* = \dot{\gamma}^{*1-m}(1+\dot{\gamma}^*)^m,$$

where u_M^* is the maximum reduced velocity on the axis of the tube. A diagram derived from the computations of Lasvergères & Lanchon (1962) is shown in figure 6.

Once the flow rate q and the characteristic parameters m, τ_∞ and μ_∞ of the liquid are known, one can obtain $\tilde{f}$ from figure 5. In figure 6, the ordinate corresponding to $\frac{1}{8}\tilde{f}$ is u_M^*. It is now possible to draw the true velocity profile.

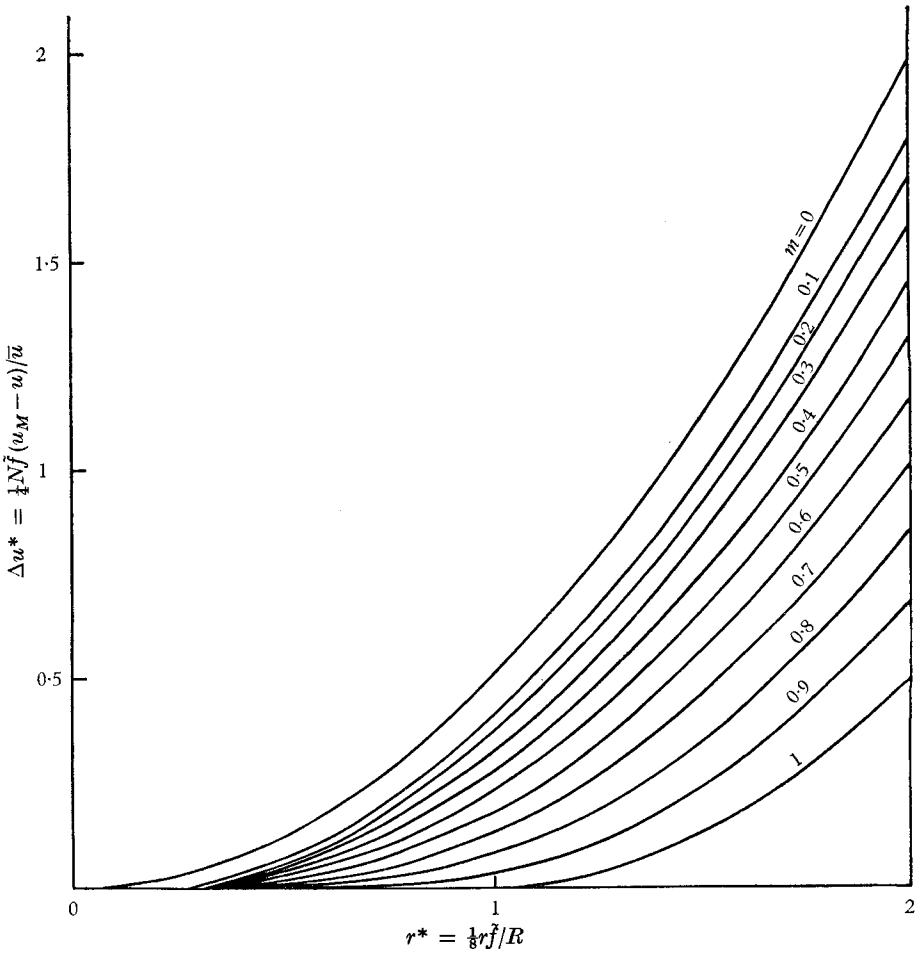

FIGURE 6. Calculated profile for the reduced velocity defect (Δu^*, r^*).

Comparison with experiment

The laboratory apparatus consisted of horizontal, cylindrical, smooth tubes of steel or glass. Their internal diameter was accurately determined by measuring the loss of head when a Newtonian fluid of known viscosity (glycerine solution) was made to flow through it. Three equidistant 0·5 cm I.D. pressure taps were provided at right angles to the axis of the tube. The tubes had sharp-edged entrances and the distance of the first tap from the entrance was at least 50 tube diameters. As maintained by Bogue (1960), this length appeared to be satisfactory for measuring asymptotic pressure gradients in laminar or turbulent flow, whether Newtonian or non-Newtonian.

Table 1 gives the dimensions of the tubes, including entrance length and position of pressure taps.

The mud was circulated through the tube:

(*a*) by a centrifugal pump, when the flow rate was high;

(*b*) by gravity from a vessel fed by the pump;

(*c*) by lowering the pressure in a vessel situated downstream, the upstream reservoir being at atmospheric pressure (figure 7).

The last two methods were used when the flow rate was low.

The pressure differences between the first and the second tap and between the second and the third tap were measured by two U-tubes filled with carbon tetrachloride, bromoform or mercury. In the latter case, carbon tetrachloride was used as an intermediary liquid between the mud and the mercury. When the

	Diameter (cm)	Total length (cm)	Dimensions downstream to entrance (cm)		
			Tap 1	Tap 2	Tap 3
Glass tubes	0·3	200	25	100	175
	0·57	200	35	105	175
	1·0	200	55	115	175
Steel tubes	1·2	600	75	300	525
	1·6	600	85	300	515
	2·0	600	100	300	500
	2·6	600	150	300	450

TABLE 1

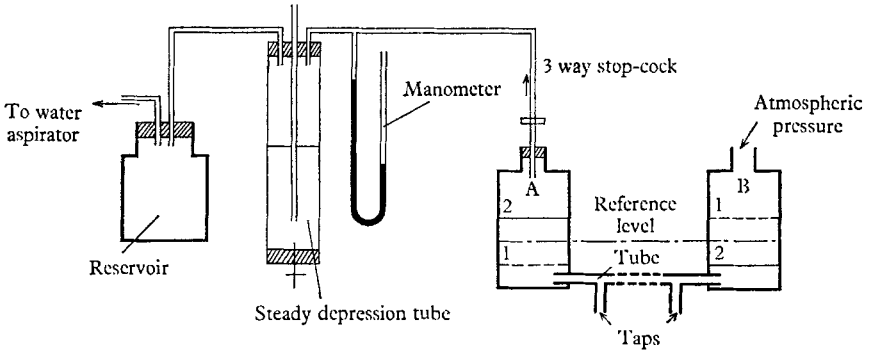

FIGURE 7. Diagram of the apparatus with lowered downstream pressure.

flow rate was high, it was measured by a Foxboro electromagnetic flow meter whose calibration had first been checked with a Newtonian fluid (water) as well as a non-Newtonian liquid (bentonite suspension). When the flow rate was low, we weighed the volume of fluid which had been discharged into a weigh tank for a given time. In the arrangement with two vessels (figure 7) we measured the time taken to fill the calibrated volume between levels 1 and 2 in vessel A or B. It was decided that the difference between levels 1 and 2 should be so small that the variation of pressure during the measurement could be neglected. All the measurements were made at ambient temperature. The variations of room temperature during the course of an experiment were so slight that the rheological characteristics were constant.

In figure 8, as an example, we have plotted the experimental points in the form of a graph of $\log f$ vs. $\log N$. It is seen that the points trace a single curve regard-

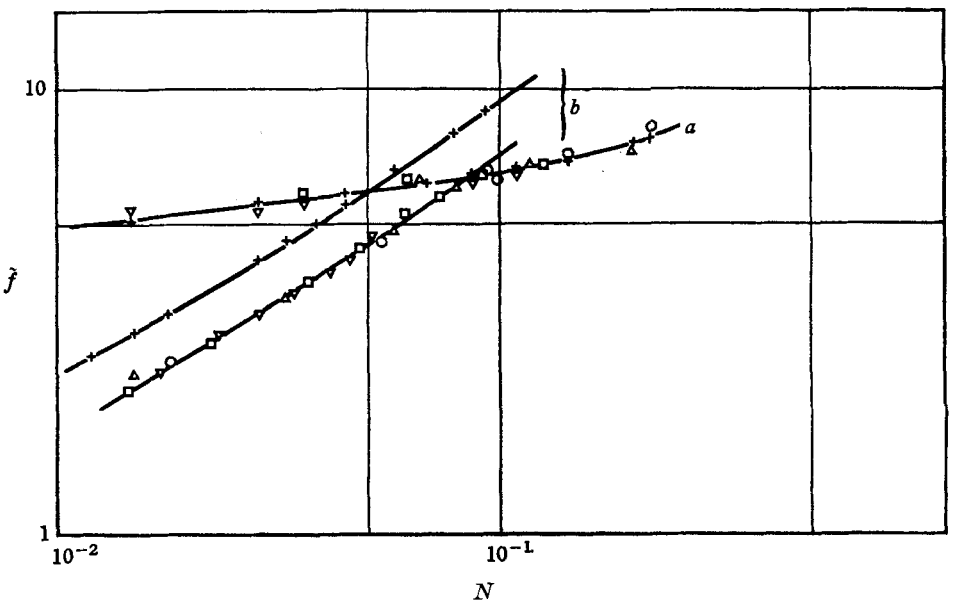

FIGURE 8. Experimental curves representing losses for two drilling muds. a — $m = 0{\cdot}9$, $\tau_\infty = 12{\cdot}95$ N/m², $\mu_\infty = 0{\cdot}0026$ Pl; b — $m = 0{\cdot}5$, $\tau_\infty = 14$ N/m², $\mu_\infty = 0{\cdot}0217$ Pl. +, predicted points; ○, 1·2 cm I.D. pipe; △, 1·6 cm I.D. pipe; □, 2·0 cm I.D. pipe; ▽, 2·6 cm I.D. pipe.

	Rheological parameters			Coaxial-cylinder viscometers				Circular tubes	
Fluids (aqueous suspensions)	m	τ_∞ N/m²	μ_∞ Pl	$\dot{\gamma}_{min}$ s^{-1}	$\dot{\gamma}_{max}$ s^{-1}	τ_{min} N/m²	τ_{max} N/m²	τ_{Rmin} N/m²	τ_{Rmax} N/m²
Bentonite I[1]—60 g/l.	0·9	10·8	0·0026	11	2256	4·4	16·5	9·5	15·5
Bentonite II[2]—55 g/l.	1	12·6	0·004	20	2256	11·3	20·9	12	16
Bentonite + calcium chloride	0·85	3·6	0·0036	29	1950	2·5	11	4·3	9·3
Bentonite I—100 g/l. + inorganic thinner[3]	0·9	16	0·008	3	2256	11·8	31·9	13·5	25
Bentonite + inorganic thinner[3] + CMC[4]	0·5	9·3	0·019	11	2256	2·1	49	7·5	40
Bentonite + organic thinner[5] + CMC[4] + calcium chloride	0·6	2·9	0·0048	29	2500	1·3	15·4	2	10·5
Bentonite + organic thinner[5] + CMC[4] + gypsum	0·3	3·5	0·003	110	2500	5·6	87·3	4·2	82·2
Attapulgite clay	0·9	6·2	0·003	130	2500	5·6	13·7	6·1	11·8

(1) Bentonite for oil-well drilling mud.
(2) Bentonite for oil-well drilling mud of different manufacture.
(3) Sodium phosphate.
(4) Carboxymethylcellulose.
(5) Ferrochrome lignosulphonate.

TABLE 2. Summary of values of rheological parameters and ranges of determination (data obtained at Institut Français du Pétrole)

less of the tube diameter; in the case (*a*), this curve coincides with the calculated curve corresponding to $m = 0{\cdot}9$. Occasionally, like in the case (*b*), we noticed that the experimental curve did not coincide with the calculated one but was parallel to and slightly below it. This difference in behaviour is due to the fact that the fluid in question did not follow Briant's law exactly for the lower values of the shear velocities. In such a case it is necessary to make new measurements at lower rotation speeds and to compose a more elaborate formula than equation (1) involving four or even more parameters.

	Rheological parameters			Circular tubes	
Fluids	m	τ_∞ N/m²	μ_∞ Pl	$\tau_{R\min}$ N/m²	$\tau_{R\max}$ N/m²
(1) Cement rock slurry	1	5·12	0·0028	4·6	7·3
(2) ThO_2 suspension	1	33·1	0·0057	45	100
(3) ThO_2 suspension	0·9	77·8	0·0075	55	195
(4) Lime suspension	0·9	23	0·00512	12·5	62·5
(5) Attasol suspension (11·8%)	0·7	142	0·0026	22·5	263
(6) Attasol suspension (13%)	0·7	330	0·0038	42·5	332
(7) Sewage sludge	1	3·73	0·03	32·3	47
(8) Sewage sludge	1	0·8	0·056	10·8	18·1

(1) Wilhelm, Wroughton & Loeffel (1939). (5)–(6) Dodge (1958).
(2)–(3) Thomas (1962). (7)–(8) Cadwell & Babbitt (1941).
(4) Alves, Boucher & Pigford (1952).

TABLE 3. Summary of values of rheological parameters and ranges of determination (data from literature)

In the following, we have restricted our investigation to the group of fluids showing agreement between experimental and calculated head-losses curves. Table 2 gives the values of the rheological parameters m, τ_∞ and μ_∞ for this group of fluids. Ranges of values obtained with coaxial cylinder viscometers (minimum and maximum values of shear velocities and shear stresses) and with circular tubes (minimum and maximum values of wall shear stresses) are also given. Table 3 shows the values of the rheological parameters deduced from head-losses data obtained by previous authors on several different fluids.

3. Transition of the flow

The Ryan & Johnson criterion

It is well known that laminar flow in a pipe becomes turbulent at a certain critical flow rate. When the fluid is Newtonian and the conduit circular, transition occurs at a Reynolds number which varies slightly with the perturbation level in flow but which has a mean value of 2100. In the case of a non-Newtonian fluid, one can deduce from dimensional analysis that the transition will occur at a value (of the generalized Reynolds number) which is a function of the generalized Hedström number. But we have no reasons to think that this function would be a constant.

Since, at present, there exists no theory of transition, different authors have turned to empirical criteria of transition (Metzner 1956; Ryan & Johnson 1959).

It has been shown by Hanks & Christiansen (1962) that Metzner's criterion (friction factor f equal to 3×10^{-2}) does not apply very well when the fluid cannot be considered of the power-law type. We have therefore employed the criterion proposed by Ryan & Johnson (1959) in order to estimate the conditions for transition in non-Newtonian fluids in circular tubes. In this case, one assumes that the flow is turbulent if the dimensionless function

$$Z(r) = -\frac{R\rho u}{\tau_R}\frac{du}{dr} \tag{25}$$

attains values in excess of 808. The flow rate corresponding to transition will then be that for which *the maximum value of* $Z(r)$ *is equal to* 808. This value was chosen so that the Reynolds number would be equal to 2100 for a Newtonian fluid (parabolic velocity profile).

An interpretation of this empirical criterion has been given by Hanks (1963). The Z function is proportional to the local ratio of a part of the inertial terms $|\rho \mathbf{V} \wedge \operatorname{curl} \mathbf{V}|$ and of the viscous term $|\operatorname{div} \boldsymbol{\tau}|$ in the momentum equations, when $\mathbf{V}$ is the velocity and $\boldsymbol{\tau}$ the deviatoric stress tensor. In the case of a circular pipe, $\rho \mathbf{V} \wedge \operatorname{curl} \mathbf{V}$ is a vector in the radial direction and $\operatorname{div} \boldsymbol{\tau}$ is a vector in the axial direction. The value of the latter is equal to

$$\frac{1}{r}\frac{d(r\tau)}{dr}.$$

We can calculate $Z(r)$ from the parametric equations (14) for u. Hence

$$Z(\dot{\gamma}^*) = (2He/m\tilde{f})\,\dot{\gamma}^*\dot{\gamma}_R^{*m-1}(1+\dot{\gamma}_R^*)^{-m}[P(\dot{\gamma}_R^*) - P(\dot{\gamma}^*)].$$

The maximum of Z is obtained for a value of r such that $dZ/dr = 0$. This condition can be expressed in the equivalent form $dZ/d\dot{\gamma}^* = 0$, since the function $\dot{\gamma}^*(r^*)$ is monotonically increasing. Since

$$dZ/d\dot{\gamma}^* = (2He/m\tilde{f})\,\dot{\gamma}_R^{*m-1}(1+\dot{\gamma}_R^*)^{-m}\,[P(\dot{\gamma}_R^*) - P(\dot{\gamma}^*) - (1-m+\dot{\gamma}^*)\,(1+\dot{\gamma}^*)^{m-1}/\dot{\gamma}^{*m-2}], \tag{26}$$

the value of $\dot{\gamma}_m^*$ which makes $dZ/d\dot{\gamma}^* = 0$ will then be the solution of the equation

$$P(\dot{\gamma}_R^*) = P(\dot{\gamma}_m^*) + (1-m+\dot{\gamma}_m^*)\,(1+\dot{\gamma}_m^*)^{m-1}/\dot{\gamma}^{*m-2}; \tag{27}$$

hence it is a function of $\dot{\gamma}_R^*$.

When the maximum of Z is equal to 808, the reduced pressure gradient $\tilde{f}$ must be given by the following expression:

$$\tilde{f} = (mHe/404)\,\dot{\gamma}_m^*\dot{\gamma}_R^{*m-1}(1+\dot{\gamma}_R^*)^{-m}[P(\dot{\gamma}_R^*) - P(\dot{\gamma}_m^*)]. \tag{28}$$

If, in figure 5, $\log \tilde{f}$ vs. $\log N$, a curve is drawn with

$$N = \frac{\dot{\gamma}_R^*}{6} - \frac{\dot{\gamma}_R^*}{6(4-3m)\,(1+\dot{\gamma}_R^*)^4}\,{}_2F_1\left(5, 4-3m; 5-3m; \frac{\dot{\gamma}_R^*}{1+\dot{\gamma}_R^*}\right) \tag{29}$$

for the abscissa and the value of $\tilde{f}$ given by (28) for the ordinate, the intersection of this auxiliary curve with the curve of the parametric expressions (24), which corresponds to the head drop in laminar flow, will be the point representing transition in the flow.

The Reynolds number of transition, Re_t, is expressed as a function of He by the following parametric equations:

$$\left.\begin{aligned} Re_t &= 50{\cdot}5\,\frac{\dot\gamma_R^{*2(1-m)}(1+\dot\gamma_R^*)^{2m}\dot\gamma_m^{*m-3}}{(1-m+\dot\gamma_m^*)\,(1+\dot\gamma_m^*)^{m-1}}\left\{\frac{\dot\gamma_R^*}{6}-\frac{\dot\gamma_R^*}{6(4-3m)\,(1+\dot\gamma_R^*)^4}\right.\\ &\qquad\left.\times\,{}_2F_1\left(5,4-3m;5-3m;\frac{\dot\gamma_R^*}{1+\dot\gamma_R^*}\right)\right\},\\ He &= 50{\cdot}5\,\frac{\dot\gamma_R^{*2(1-m)}(1+\dot\gamma_R^*)^{2m}\dot\gamma_m^{*(m-3)}}{(1-m+\dot\gamma_m^*)\,(1+\dot\gamma_m^*)^{m-1}}, \end{aligned}\right\} \tag{30}$$

in terms of the parameter $\dot\gamma_R^*$. Curves representing $\log Re_t$ as a function of $\log He$ are shown in figure 9. When $m = 0$, it is clear that $Re_t = 2100$. When $m = 1$, one obtains the curves previously calculated by Hanks (1963) for a Bingham body. It is observed that all the representative curves for $0 < m < 1$ do not lie entirely between the curves for $m = 0$ and $m = 1$. This explains why Hanks (1963) found that certain experimental points were above the curve corresponding here to $m = 1$, since these points should belong to fluids whose plasticity parameter m is closer to 0·9 than to 1. The discrepancy is seen to be more pronounced in the figure given by Hanks, since its value of He is referred to the asymptotic Bingham body and is equal here to mHe, as defined by equation (20).

Comparison with experiment

We present here some experimental results on the transition from laminar to turbulent régime for several fluids obeying the Briant equation, the flow still being in tubes with circular cross-section. These results were deduced either from published data obtained with fluids of widely varying composition or from measurements made at the Institut Français du Pétrole, especially with drilling muds.

In all the cases considered, the transition flow rate is that which corresponds to the end of the laminar and not to the beginning of the fully turbulent flow, if the extent of the transition zone is appreciable. In figure 10, for instance, representative points for the laminar and turbulent flows of a drilling mud are plotted. All laminar points are located on the same curve. The turbulent points are on different straight lines corresponding to different Hedström numbers. Thus, the abscissae of the kinks give us the values of the transition Reynolds number as a function of the Hedström number.

Figure 11 shows the correlation between the values of $(Re_t)_{\text{calc}}$ given by the Ryan & Johnson criterion and the values $(Re_t)_{\text{exp}}$ obtained by experiment. The agreement between them seems satisfactory.

Practical use of the transition diagram

In practical cases, the diagram in figure 9 can be used to ascertain the nature of the flow, particularly when design calculations are made to determine the loss of head for pump dimensioning. If a given flow rate is prescribed, and the pipe diameter has not yet been determined, the characteristic operating point (He, Re) is located on a straight line with a slope equal to $-\frac{1}{2}$. This straight line cuts

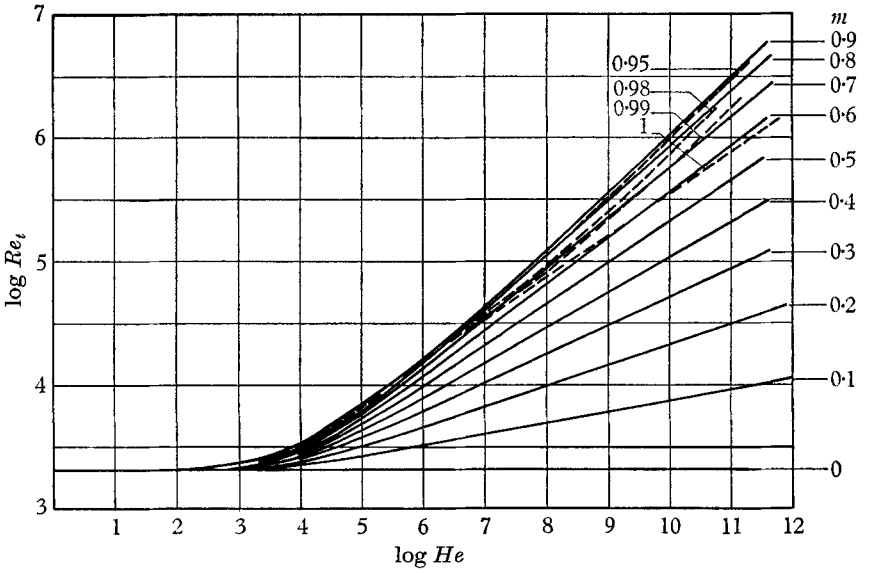

FIGURE 9. (log Re_t, log He) calculated for different values of m.

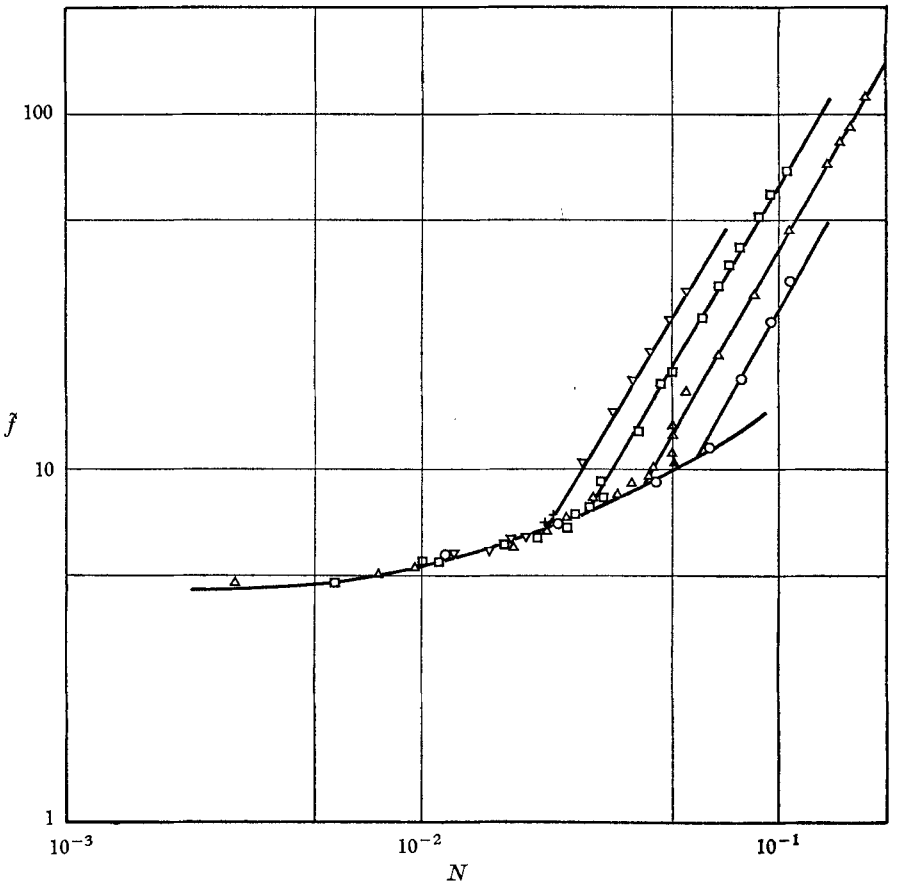

FIGURE 10. Experimental curves representing losses for a bentonite suspension (m = 0·9, τ_∞ = 5·15 N/m², μ_∞ = 0·0042 Pl) in laminar and turbulent flow. ▽, 2·6 cm I.D. pipe ($He = 2{\cdot}24 \times 10^5$); □, 2·0 cm I.D. pipe ($He = 1{\cdot}46 \times 10^5$); △, 1·6 cm I.D. pipe ($He = 7{\cdot}96 \times 10^4$); ○, 1·2 cm I.D. pipe ($He = 4{\cdot}6 \times 10^4$).

the transition curve corresponding to the fluid plasticity parameter at a point corresponding to a diameter D_t. For diameters smaller than D_t, the flow will be turbulent and the losses must not be computed with the aid of figure 5. One must then have recourse to direct experimental results.

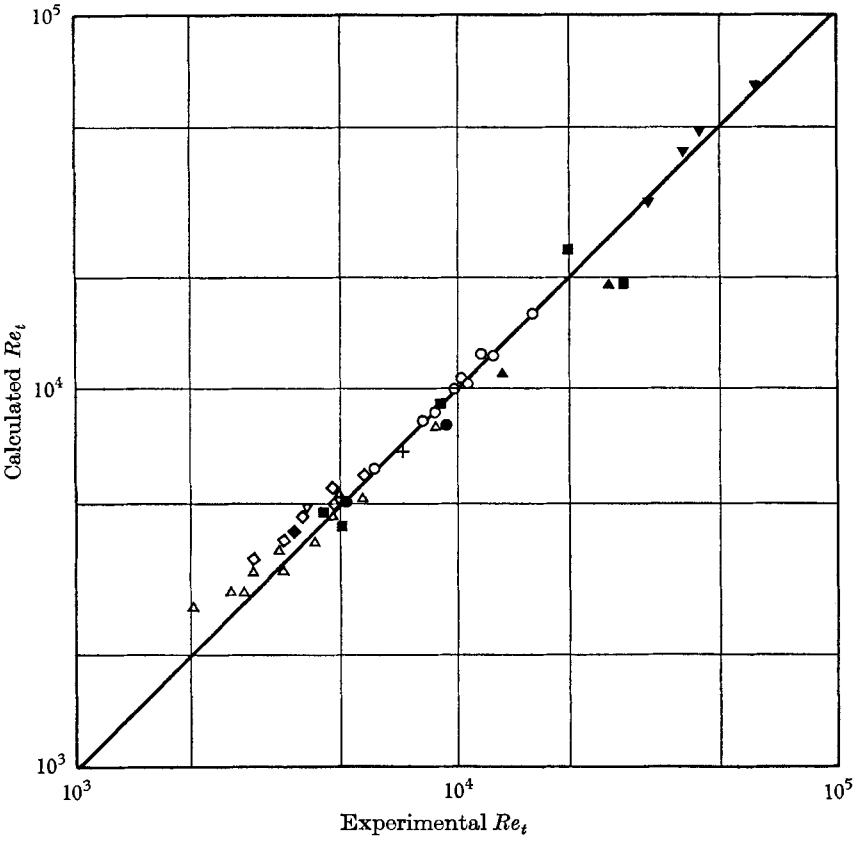

FIGURE 11. Comparison between calculated transition Reynolds number $(Re_t)_{calc}$ and experimental transition Reynolds number $(Re_t)_{exp}$. ▲, cement rock slurry (Wilhelm, Wroughton & Loeffel 1939); ■, ThO_2 suspension (Thomas 1962); ●, lime suspension (Alves, Boucher & Pigford 1952); ▼, Attasol suspension (Dodge 1958); ◆, sewage sludge (Cadwell & Babbitt 1941); +, clay suspension (Cadwell & Babbitt 1941); values obtained at Institut Français du Pétrole: ○, bentonite suspensions; △, bentonite + CMC + barite suspension; ◇, red tannin drilling mud.

4. Conclusions

It has been found that the rheological behaviour of a lot of suspensions and some drilling muds can be conveniently represented by a formula with only three parameters. The Ostwald–De Waele and Bingham laws are particular cases of this general law.

This formula has also been used to extrapolate at the lower shear stresses which are difficult to measure on conventional viscometers. The accuracy of such extrapolation has been proved by the agreement between experimental and calculated head losses in circular tubes.

For the transition flow rate, an empirical transition criterion first proposed by Ryan & Johnson has been adopted to compute the relationship between two non-dimensional numbers, viz. the generalized Reynolds and Hedström numbers. The experimental and the calculated transition Reynolds numbers appear to agree quite well and demonstrate that the Ryan & Johnson criterion may possess a hidden but fundamental justification.

REFERENCES

ALVES, G. E., BOUCHER, R. L. & PIGFORD, R. L. 1952 Pipe line design for non Newtonian solutions and suspensions. *Chem. Engng Progr.* **48**, 385–93.

BOGUE, D. C. 1960 Velocity profiles in turbulent non-Newtonian pipe flow. Ph.D. Thesis, Univ. of Delaware (Univ. Microfilms, Inc. Ann Arbor), pp. 27–9.

BRIANT, J. 1956 Etude des propriétés rhéologiques des graisses à l'aide du viscosimètre S.O.D. *Rev. Inst. Franç. Pétrole*, **11**, 113–33; 247–87.

CADWELL, D. W. & BABBITT, H. E. 1941 Flow of muds, sludges and suspensions in circular pipe. *Trans. A.I.Ch.E.* **37**, 237–66.

CASSON, N. 1959 A flow equation for pigment–oil suspensions of the printing ink type. In *Rheology of disperse systems*. Ed. C. C. Mill, pp. 84–104. London: Pergamon Press.

DODGE, D. W. 1958 Turbulent flow of non-Newtonian fluids in smooth round tubes. Ph.D. Thesis, Univ. of Delaware.

HANKS, R. W. 1963 The laminar turbulent transition for fluids with a yield stress. *A.I.Ch.E. J.* **9**, 306–9.

HANKS, R. W. & CHRISTIANSEN, E. B. 1962 The laminar turbulent transition in non-isothermal flow of pseudoplastic fluids in tubes. *A.I.Ch.E. J.* **8**, 467–71.

HERSCHEL, W. H. & BULKLEY, R. 1926 Konsistenzmessungen von Gummi-Benzollösungen. *Kolloid Z.* **39**, 291–300.

KRIEGER, I. M. & MARON, S. H. 1954 Direct determination of the flow curve of non-Newtonian fluids. III. Standardized treatment of viscometric data. *J. Appl. Phys.* **25**, 72–5.

LASVERGÈRES, J. M. & LANCHON, M. 1962 Résolution numérique de l'équation d'écoulement d'un fluide non-Newtonien dans un tube capillaire. *Rapp. Inst. Franç. Pétrole*, no. 7151.

MARTIN, M. & LE FUR, B. 1963 Etude de l'écoulement laminaire d'un fluide non-Newtonien dans un tube de section circulaire. Application aux boues de forage. *Rev. Inst. Franç. Pétrole*, **18**, N° hors-série, 32.

MELROSE, J. C. & LILIENTHAL, W. B. 1951 Plastic flow properties of drilling fluids—measurement and application. *J. Petroleum Tech.* **192**, 159.

METZNER, A. B. 1956 Non-Newtonian technology: fluid mechanics, mixing and heat transfer. *Adv. Chem. Engng.* **1**, 77–153.

POWELL, R. E. & EYRING, H. 1944 Mechanism for relaxation theory of viscosity. *Nature, Lond.* **154**, 427–8.

PRAGER, W. 1961 *Introduction to Mechanics of Continua*, p. 141. Chicago: Ginn and Co.

RYAN, N. W. & JOHNSON, M. M. 1959 Transition from laminar to turbulent flow in pipes. *A.I.Ch.E. J.* **5**, 433–5.

SISKO, A. W. 1958 The flow of lubricating greases. *Ind. Engng Chem.* **50**, 1789.

THOMAS, D. G. 1962 Transport characteristics of suspensions: Part IV. Friction loss of concentrated–flocculated suspensions in turbulent flow. *A.I.Ch.E. J.* **8**, 266–71.

WILHELM, R. H., WROUGHTON, D. M. & LOEFFEL, W. F. 1939 Flow of suspensions through pipes. *Ind. Engng. Chem.* **31**, 622–7.